PERGAMON

International Journal of Solids and Structures 37 (2000) 2673–2694

INTERNATIONAL JOURNAL OF SOLIDS and STRUCTURES

www.elsevier.com/locate/ijsolstr

Effect of material nonlinearity in unidirectional composites on the behavior of beam structures

G.A. Abu-Farsakh*, S.A. Barakat, N.R. Al-Zoubi

Civil Engineering Department, Jordan University of Science & Technology, PO Box 3030, Irbid, Jordan

Received 3 March 1998; received in revised form 25 January 1999

Abstract

The present study is made to investigate the effect of material nonlinearity in unidirectional composites on the behavior of beams, where the fiber orientation is considered. The effect of these two factors on deflection, bending moment and external reactions is investigated. In order to achieve these objectives, a computer subroutine based on secant mechanical property is incorporated in a main computer program for beam and frame analysis. The program can solve structures made of unidirectional composite materials which exhibit general material nonlinearity. Several numerical examples including various beam structures having different fiber orientations are presented, for both linear and nonlinear analysis.

1. Introduction

Composite materials or so called advanced materials will partially replace conventional materials in civil engineering structures, due to many advantages that distinguish them over the conventional materials like higher strength and stiffness to weight ratios, better corrosion and wear resistance in addition to many other advantages (Jones, 1975). Hence, due to this growing importance of composite materials in the last decade, the necessity of understanding the behavior of those materials has also increased. An important aspect in this field is the material nonlinearity and its effect on the overall structural behavior.

Although beams and columns are the most commonly used structural elements, most of the studies and theories in the literature which deal with material nonlinearity effect in composite structures are applied to plates or shells.

Material nonlinearity as a general term was studied by many investigators. Philip and Karen (1988) approximated the actual material behavior as a multilinear load-deformation model where the material

* Corresponding author.
E-mail address: ghazi@just.edu.jo (G.A. Abu-Farsakh).

0020-7683/00/$ - see front matter
PII: S0020-7683(99)00039-6

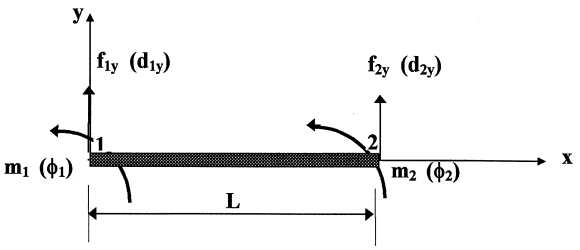

Fig. 1. Nodal displacements and nodal forces acting on beam element.

was assumed to follow a bilinear force-deformation relationship. Prokic's approach (Prokic, 1994) to the solution was based on the finite-element method using incremental solution techniques. Cheung et al. (1989) dealt with the elasto–plastic material case using the finite strip method.

Other investigators dealt with both material and geometric nonlinearities. Wong and Tin-Loi (1990) used a path linearization strategy to directly link a geometrically nonlinear formulation to small displacement elasto–plastic analysis of frame structures. Meek and Loganathan (1990) used an incremental-iterative method based on the arc length method combined with the Newton–Raphson method to solve the non-linear governing equations in order to analyze the large displacement analysis of elasto–plastic frame structures. Meek and Lin (1990) studied the geometric and material nonlinearities of thin-walled beam-columns where the effective stress–strain curve is determined experimentally.

When beams made of composite materials are concerned, Vinson and Sierakowski (1986) applied the classical lamination theory along with the plane strain assumption to obtain the extentional, coupling and bending stiffness for an Euler–Bernoulli type laminated beam. Fuh-Gwo and Miller (1989) produced a finite element model that can be used for laminated beams. The model includes separate rotational degrees of freedom for each lamina. A general finite element with ten degrees of freedom was derived by Wu and Sun (1990) for thin-walled laminated composite beams. Barbero et al. (1993) presented a formal engineering approach for the mechanics of thin-walled laminated beams based on the kinematic assumption and consistent with Timishinko beam theory.

2. Objectives

The present study is aimed to investigate the effect of material nonlinearity in unidirectional composites on the behavior of beam structures, where the fiber orientation and the nonlinear stress–strain behavior are considered. The effect of these two factors on deflection, bending moments and reactions of structures are investigated.

3. Finite element formulation

A typical beam element consisting of two nodes is used in the problem formulation as shown in Fig. 1. Each node has two degrees of freedom; one translation (d_{iy}) and one rotation (ϕ_i), where the subscript i is the node number ($i = 1, 2$). The element local axes (x and y) are taken at node (1) as an origin where x-axis coincides with the element axis and y is the perpendicular axis. The rotation is considered positive in the counterclockwise direction. The transverse displacement function (v) is assumed to vary cubically with respect to x, such that:

$$v(x) = a_1x^3 + a_2x^2 + a_3x + a_4. \tag{1}$$

In terms of nodal displacements (degrees of freedom, d.o.f.) the displacement function is given as:

$$v = [N_1, N_2, N_3, N_4]\begin{Bmatrix} d_{1y} \\ \phi_1 \\ d_{2y} \\ \phi_2 \end{Bmatrix} \tag{2}$$

or, alternatively,

$$v = [N]\{d\} \tag{3}$$

where, N_i's are defined as the displacement shape functions and are represented as:

$$N_1 = \frac{1}{L^3}(2x^3 - 3x^2L + L^3)$$

$$N_3 = \frac{1}{L^3}(-2x^3 + 3x^2L)$$

$$N_2 = \frac{1}{L^3}(x^3L - 2x^2L^2 + xL^3)$$

$$N_4 = \frac{1}{L^3}(x^3L - x^2L^2). \tag{4}$$

The axial strain (ε_x) is related to the displacement function as follows:

$$e_x(x, y) = -y\frac{\mathrm{d}^2v}{\mathrm{d}x^2}. \tag{5}$$

From elementary beam theory, the bending moment (M) and the shear force (V) are related to the transverse displacement function as:

$$M = EI\frac{\mathrm{d}^2v}{\mathrm{d}x^2} \tag{6}$$

and

$$V = EI\frac{\mathrm{d}^3v}{\mathrm{d}x^3} \tag{7}$$

where, EI is the flexural stiffness of the beam element.

Considering the nodal and beam sign conventions for shear forces and bending moments using Eqs. 3–7, we obtain:

$$f_{1y} = V = EI\frac{\mathrm{d}^3v(0)}{\mathrm{d}x^3} = \frac{EI}{L^3}(12d_{1y} + 6L\phi_1 - 12d_{2y} + 6L\phi_2)$$

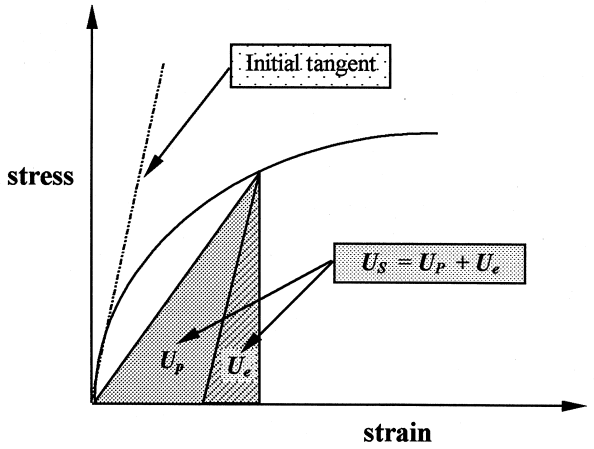

Fig. 2. Typical nonlinear stress–strain curve for the ith mechanical property showing the energy terms.

$$m_1 = -M = -EI\frac{\mathrm{d}^2 v(0)}{\mathrm{d}x^2} = \frac{EI}{L^3}(6Ld_{1y} + 4L^2\phi_1 - 6Ld_{2y} + 2L^2\phi_2)$$

$$f_{2y} = -V = -EI\frac{\mathrm{d}^3 v(L)}{\mathrm{d}x^3} = (-12d_{1y} - 6L\phi_1 + 12d_{2y} - 6L\phi_2)$$

$$m_2 = M = EI\frac{\mathrm{d}^2 v(L)}{\mathrm{d}x^2} = \frac{EI}{L^3}(6Ld_{1y} + 2L^2\phi_1 - 6Ld_{2y} + 4L^2\phi_2). \tag{8}$$

In matrix form, Eq. 8 appears as:

$$\begin{Bmatrix} f_{1y} \\ m_1 \\ f_{2y} \\ m_2 \end{Bmatrix} = \frac{EI}{L^3}\begin{bmatrix} 12 & 6L & -12 & 6L \\ 6 & 4L^2 & -6L & 2L^2 \\ -12 & -6L & 12 & -6L \\ 6L & 2L^2 & -6L & 4L^2 \end{bmatrix}\begin{Bmatrix} d_{1y} \\ \phi_1 \\ d_{2y} \\ \phi_2 \end{Bmatrix} \tag{9}$$

or, in short matrix form as:

$$\{f\} = [k]\{d\} \tag{10}$$

where $\{f\}$ is the nodal forces vector, $\{d\}$ is the nodal displacements vector and $[k]$ is the local element stiffness matrix.

4. Composite material model

Unidirectional composites are, generally, characterized by their nonlinear stress–strain response. Therefore, the element stiffness matrix $[K]$ can not be used directly, and a new approach has to be used to deal with the material nonlinearity problem. The present approach incorporates the secant modulus E_s into the stiffness matrix of the beam element instead of the ordinary elastic modulus E_0.

For the purpose of calculating E_s for a given lamina, a new material model developed by Abu-Farsakh (1989) is used. In this model the mechanical property expression is a function of the plastic

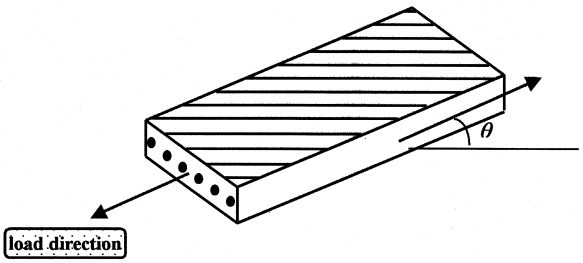

Fig. 3. Typical unidirectional composite lamina with fiber orientation θ.

strain energy density U_p of an equivalent linear elastic system:

$$E_{is} = E_{io}[1 - B_i(U_p/U_{io})^{Ci} + D_i(U_p/U_{io})] \quad i = 1, 2, 12 \tag{11}$$

where, E_{is} is the secant mechanical property, E_{io} is the initial value of mechanical property, B_i, C_i and D_i are the mechanical property constants and are determined by specifying three sampling points on the ith uniaxial stress–strain curve derived from the uniaxial experimental data. The quantity U_{io} is introduced for dimensional purpose and is used to non-dimensionalize the plastic strain energy density U_p. For example, considering the experimental (σ_1–ε_1) curve, where, σ_1 is the normal stress in the fiber direction and ε_1 is the normal strain in the same direction. Taking several sampling points on the curve (say 8 points). The mechanical property in this case will be:

$$E_{1s} = E_{1o}[1 - B_1(U_p)^{C1} + D_1(U_p)]. \tag{12}$$

This equation requires determination of three constants (B_1, C_1, and D_1), in which case, it requires three sampling points. Because, number of points considered are more than three, hence, a least-square fit technique of Eq. (12) is adopted in order to obtain the best curve fitting. The first and final points should be considered in all cases, where, the end of the linear part of the curve is considered as point (1) while the ultimate stress (at failure) is considered as point (8). For more details on the subject refer to Abu-Farsakh (1989).

The plastic strain energy density U_p shown in Fig. 2 is expressed as follows:

$$U_p = U_s - U_e. \tag{13}$$

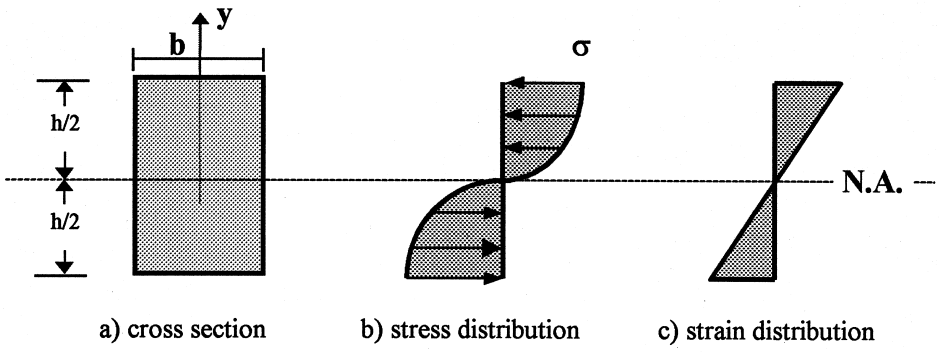

Fig. 4. Stress and strain distributions through the cross section depth.

where, U_s is the total strain energy density of an equivalent linear elastic system and U_e is the elastic strain energy density. The model calculates the secant mechanical property at a given stress level for a specified unidirectional composite with fiber orientation θ, see Fig. 3.

4.1. Stress and strain representation across the section

To account for the nonlinear material behavior across the element section (Fig. 4(a)), the stress distribution is assumed to have a cubic variation (Fig. 4(b)), such as:

$$\sigma = \alpha y^3 + by^2 + cy + d \tag{14}$$

where, *a, b, c* and *d* are constants, depending on the stress level at which the specified cross section is considered, and y is the distance through cross-sectional depth. The selection of this polynomial to represent the stress distribution across the section is due to the fact that the best fit to the stress–strain data (provided by the Abu-Farsakh, 1989 model and also due to Cole and Pipes, 1973) especially, at higher stress levels. At lower stress levels the stress variation across the depth of the section may have a lower order polynomial representations. The strain distribution through the section depth is assumed to be linear, see Fig. 4(c), this is to account for the original assumption that plane sections perpendicular to neutral axis (N.A.) before bending remain plane and perpendicular after bending.

4.2. Fiber-orientation effect

The following is the general iterative procedure used to solve the resulting nonlinear strain equations at a specified stress level.

1. Calculate stress (σ_x) at extreme fiber as an average of the two end nodal values which correspond to a certain load level on the beam.
2. Determine the corresponding stresses in the principal material direction using the following transformation relations:

$$\sigma_1 = \sigma_x \cos^2\theta$$

$$\sigma_2 = \sigma_x \sin^2\theta$$

$$\tau_{12} = -\sigma_x \sin\theta \cos\theta \tag{15}$$

   where, θ is the fiber orientation angle.
3. Determine the plastic strain energies:

$$U_{p_1} = \frac{\sigma_1^2}{2E_{1s}} - \frac{\sigma_1^2}{2E_{1o}}$$

$$U_{p_2} = \frac{\sigma_2^2}{2E_{2s}} - \frac{\sigma_2^2}{2E_{2o}}$$

$$U_{p_{12}} = \frac{\tau_{12}^2}{2G_{12s}} - \frac{\tau_{12}^2}{2G_{12o}}$$

$$U_{\mathrm{p}} = U_{\mathrm{p}_1} + U_{\mathrm{p}_2} + U_{\mathrm{p}_{12}} \tag{16}$$

(a) For a linear elastic material $U_{\mathrm{p}} = 0$, which corresponds to

$$E_{1\mathrm{s}} = E_{1\mathrm{o}},\ E_{2\mathrm{s}} = E_{2\mathrm{o}},\ G_{12\mathrm{s}} = G_{12\mathrm{o}}. \tag{17}$$

(b) For a nonlinear material behavior, in order to allow for iterations, initial secant moduli are assigned values of:

$$E_{1\mathrm{s}} = 0.99E_{1\mathrm{o}}$$

$$E_{2\mathrm{s}} = 0.99E_{2\mathrm{o}}$$

$$G_{12\mathrm{s}} = 0.99G_{12\mathrm{o}}. \tag{18}$$

4. New values of $E_{1\,\mathrm{s}}$, $E_{2\,\mathrm{s}}$ and $G_{12\,\mathrm{s}}$ are determined using:

$$E_{1\mathrm{s}} = E_{1\mathrm{o}}[1 - B_1(U_{\mathrm{p}})^{C1} + D_1(U_p)]$$

$$E_{2s} = E_{2\mathrm{o}}[1 - B_2(U_{\mathrm{p}})^{C2} + D_2(U_{\mathrm{p}})]$$

$$G_{12\mathrm{s}} = G_{12\mathrm{o}}[1 - B_{12}(U_{\mathrm{p}})^{C12} + D_{12}(U_{\mathrm{p}})]. \tag{19}$$

Substituting Eq. 19 into Eq. 18 (step 3), a new U_{p}-value is obtained, namely U_{p_n}, while the old value is designated as U_{p_0}.

5. Repeating steps (3) and (4) inclusively, until the following convergence criterion is satisfied:

$$\left|\frac{U_{\mathrm{p}_n} - U_{\mathrm{p}_0}}{U_{\mathrm{p}_n}}\right| \leq \varepsilon \tag{20}$$

where, ε is assigned a small value of 10^{-4}.

6. Determine the final strains in the principal material directions ε_1, ε_2, and γ_{12} using the transformed compliances matrix $[S_{ij}]$, by substituting the final secant elastic moduli $E_{1\,\mathrm{s}}$, $E_{2\,\mathrm{s}}$ and $G_{12\,\mathrm{s}}$, such that:

$$\begin{Bmatrix} \varepsilon_1 \\ \varepsilon_2 \\ \gamma_{12} \end{Bmatrix} = \begin{bmatrix} S_{11} & S_{12} & S_{16} \\ S_{21} & S_{22} & S_{26} \\ S_{31} & S_{62} & S_{66} \end{bmatrix} \begin{Bmatrix} \sigma_1 \\ \sigma_2 \\ \sigma_{12} \end{Bmatrix} \tag{21}$$

where, in terms of the engineering constants, the compliances are

$$S_{11} = \frac{1}{E_1} \quad S_{21} = S_{12} = -\frac{v_{12}}{E_1} = -\frac{v_{21}}{E_2}$$

$$S_{22} = \frac{1}{E_2} \quad S_{66} = \frac{1}{G_{12}}$$

$$S_{16} = \frac{\gamma_{12}}{\varepsilon_1 E_1} \quad S_{26} = \frac{\gamma_{12}}{\varepsilon_2 E_2}$$

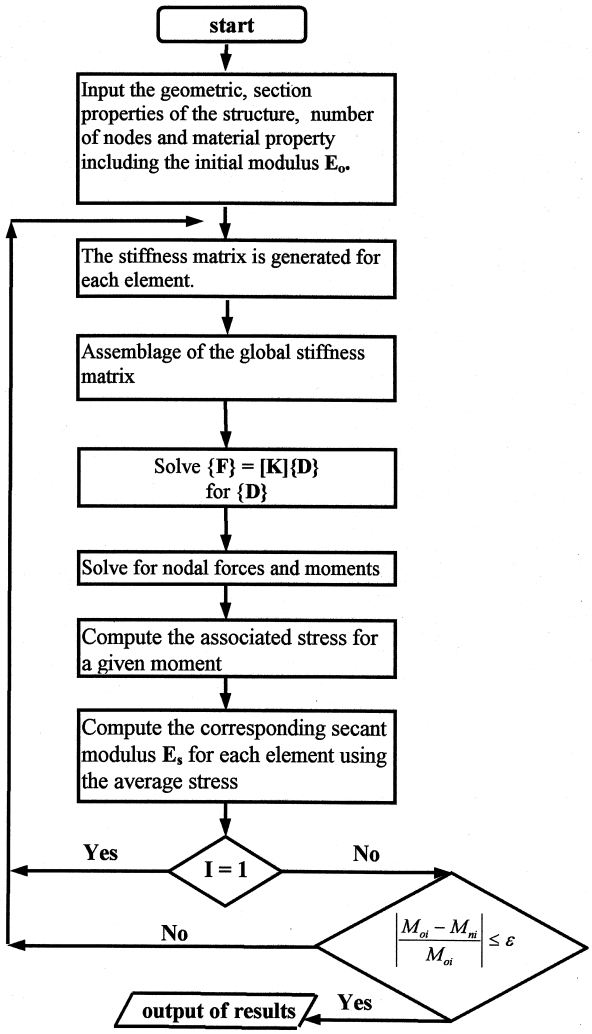

Fig. 5. A flow chart of the computer program.

7. Determine the strain ε_x, where:

$$\varepsilon_x = \varepsilon_1 \cos^2\theta + \varepsilon_2 \sin^2\theta + 2\gamma_{12} \sin\theta \cos\theta \tag{22}$$

8. Determine the secant modulus E_{xs}, such that:

$$E_{xs} = \frac{\sigma_x}{\varepsilon_x} \tag{23}$$

where, x is the geometric axis of the beam element.

9. Determine E_{xs} for each finite element repeating steps 1–8 inclusively.
10. Enter the finite element program with the secant moduli E_{xs} for each element instead of the usual elastic modulus E_0.

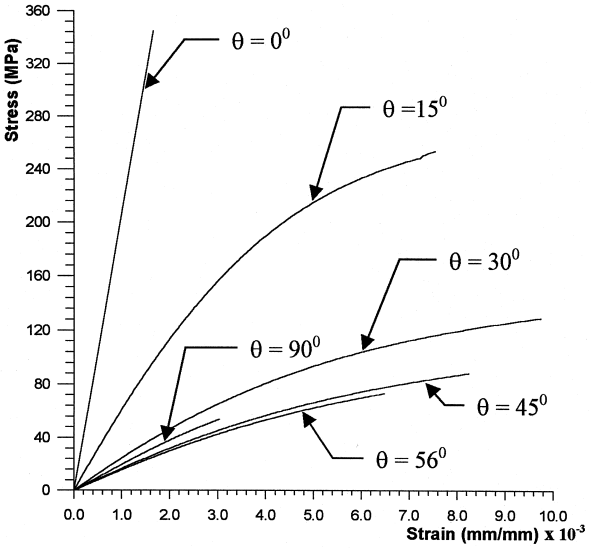

Fig. 6. Stress–strain relation for boron/epoxy lamina for different fiber orientation.

4.3. A computer program for material nonlinearity problem

In order to incorporate the secant modulus model given by Abu-Farsakh (1989) into the finite element solution, a computer program is developed. The program is capable of determining displacements, internal forces and moments for a given beam or frame structure made of unidirectional composite material such as boron/epoxy and graphite/epoxy.

The main purpose of this study is to investigate the material nonlinearity effect on the distribution of

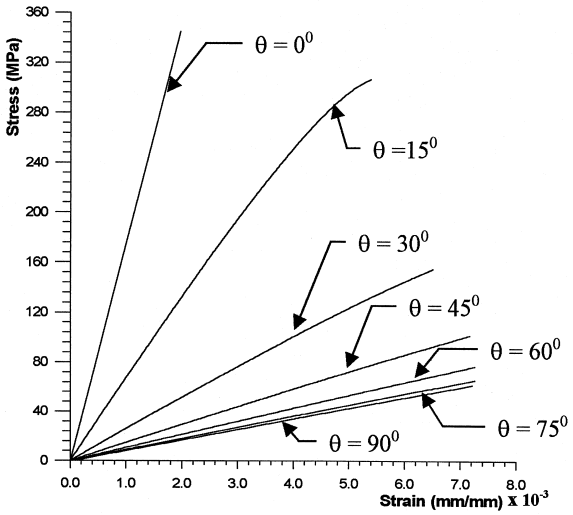

Fig. 7. Stress–strain relation for graphite/epoxy lamina for different fiber orientation.

Table 1
Material property constants (Abu-Farsakh, 1989) for boron/epoxy from uniaxial test data due to Cole and Pipes (1973)

Material property	Initial value	B_i	C_i	D_i	U_{oi}
E_1	207.54×10^3 MPa	0	1	0	1 (MPa)
E_2	19.79×10^3 MPa	0.10843	0.62186	0.01562	1 (MPa)
G_{12}	5.52×10^3 MPa	0.11515	0.42238	0.00160	1 (MPa)
v_{12}	0.225	0	1	0	1

forces and moments in beam structures. The program is originally made to analyze elements made of unidirectional composites and composed of layers having the same fiber orientation, but it can be further developed to solve structures made of multidirectional laminates.

In the present analysis, displacements are assumed to be small, stress-distribution is assumed to have a cubic variation across the section depth. Because of symmetric construction of laminates, the neutral axis (N.A.) position is considered to coincide with the middle axis (M.A.) of the cross-section. Hence, the stress-distribution is similar in both tension and compression sides. A flowchart of the computer program is shown in Fig. 5.

5. Composite material properties and behaviors

For the purpose of investigating the effect of material nonlinearity in unidirectional composites, two types of composite materials are considered in this study: boron/epoxy and graphite/epoxy. The two materials exhibit nonlinear stress–strain behavior, especially, when the load is applied off-axis to the fiber orientation (Hahn and Tsai, 1973). The degree of nonlinearity is mostly increased for angles ranging approximately between 15 and 45° (see Figs. 6 and 7), which is attributed mainly to matrix highly nonlinear shear behavior (Abu-Farsakh, 1989). After which the nonlinearity starts to decrease until it reaches a minimum at $\theta = 90°$.

Both composites are mostly used in space craft engineering because of their high strength to weight and high stiffness to weight ratios. The nonlinear behavior of the lamina is mainly attributed to the nonlinear matrix shear behavior. The mechanical property constants for uniaxial tests of boron/epoxy and graphite/epoxy laminates which are used in this study are given in Tables 1 and 2, respectively, as reported by Cole and Pipes (1973).

The stress–strain curves of boron/epoxy and graphite/epoxy laminae due to off-axis tension loading and for different fiber orientations (θ) are determined using Abu-Farsakh model (1989) and Abu-Farsakh and Abdel-Jawad (1994) and are shown in Figs. 6 and 7, respectively. It is obvious from Fig. 6 that the nonlinear behavior of boron/epoxy composite is more pronounced with increasing fiber

Table 2
Material property constants (Abu-Farsakh, 1989) for boron/epoxy from uniaxial test data due to Cole and Pipes (1973)

Material property	Initial value	B_i	C_i	D_i	U_{oi}
E_1	175.1×10^3 MPa	0	1	0	1 (MPa)
E_2	8.62×10^3 MPa	0	1	0	1 (MPa)
G_{12}	6.72×10^6 MPa	0.060648	0.23319	−0.004480	1 (MPa)
v_{12}	0.46	0	1	0	1

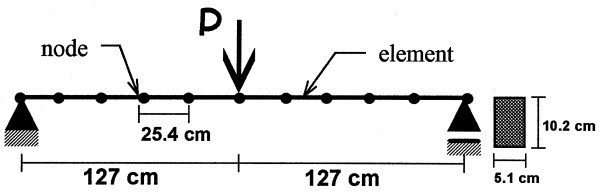

Fig. 8. Schematic representation of the geometry and loading of the simple beam.

inclination angle (θ). It is also noticed that the material stress–strain behavior softens with increasing angle (θ), up to $\theta = 56^\circ$, whereas the curve becomes stiffer with increasing (θ) afterwards. The stress–strain behavior of graphite/epoxy has less nonlinearity than that of boron/epoxy (Fig. 7), with increasing softening behavior up to $\theta = 90^\circ$.

6. Numerical examples and discussion

In this section a study of the effect of material nonlinearity and fiber orientation on the behaviors of unidirectional composite beams: deflection and bending moments, is carried out. Different types of beams, boundary conditions, and loading cases are considered. All beams considered are composed of laminates made of unidirectional composites.

6.1. Statically determinate beams

A 254 cm length simple beam is divided into 10 elements each. The cross section is 5.1×10.2 cm. The simple beam is subjected to a concentrated load acting at the middle of span, as shown in Fig. 8. The midspan deflections of the beam are determined using different loading levels for both boron/epoxy and graphite/epoxy composites, as illustrated in Fig. 9.

It can be seen in Fig. 9 that material nonlinearity affects the beam deflection. The mid-span deflections of the beam increase in an ascending manner more rapidly with increasing applied load on the beam. This point is further illustrated in Fig. 10, where two simply supported beams made of boron/epoxy laminae are incrementally loaded; the first with fiber orientation $\theta = 0^\circ$ (linear stress–strain curve, Fig. 7), and the second with $\theta = 45^\circ$ (nonlinear stress–strain curve, Fig. 7). It can be noted that in first beam ($\theta = 0^\circ$) the deflections are increased (due to incremental loading) in a linear manner, while, in the second beam ($\theta = 45^\circ$) the deflections are increased in an ascending manner attributed to the nonlinear stress–strain behavior at this angle.

Next, the effect of changing fiber orientation in simple beam on deflection is studied. The simple beam is subjected to constant load of 4.45 kN, and the resulting midspan deflection vs fiber orientation angle (θ) is plotted as shown in Fig. 11. It is clearly noted that deflections increase nonlinearly with increasing fiber orientation. However, boron/epoxy beams show different behavior from graphite/epoxy beams. With increasing fiber orientation angle (θ) from 0 to 5° in the case of boron/epoxy composite, the deflection increases slightly. Further increase of θ causes a rapid increase in deflection up to θ value of about 56°, where the stress–strain behavior becomes stiffer, and the deflection decreases, as shown in Fig. 11(b). On the other hand, the deflections of a laminated beam made of graphite/epoxy Fig. 11(c), are observed to increase slightly from 0 to 10°, while deflections increase more rapidly with increasing values of θ.

A comparison is made between the present nonlinear analysis and linear analysis using the initial

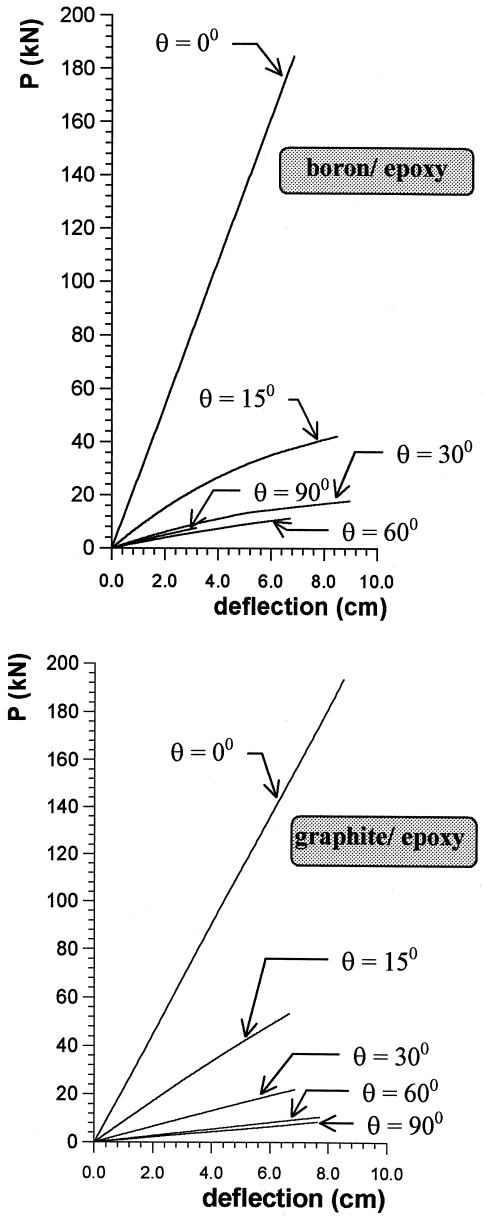

Fig. 9. Midspan deflections of the simple beams vs applied loads, for different fiber orientations (θ).

moduli of the composite materials for the beam shown in Fig. 11(a). The results are shown in Figs. 12 and 13 for boron/epoxy and graphite/epoxy, respectively. The maximum difference between the two methods is obtained at a θ approximately equals 55° for boron/epoxy, where as the maximum difference in deflections reaches about 4%, see Fig. 12(b). On the other hand, in graphite/epoxy the maximum difference occurs at a θ approximately equals 30° where it reaches a 2%, as shown in Fig. 13.

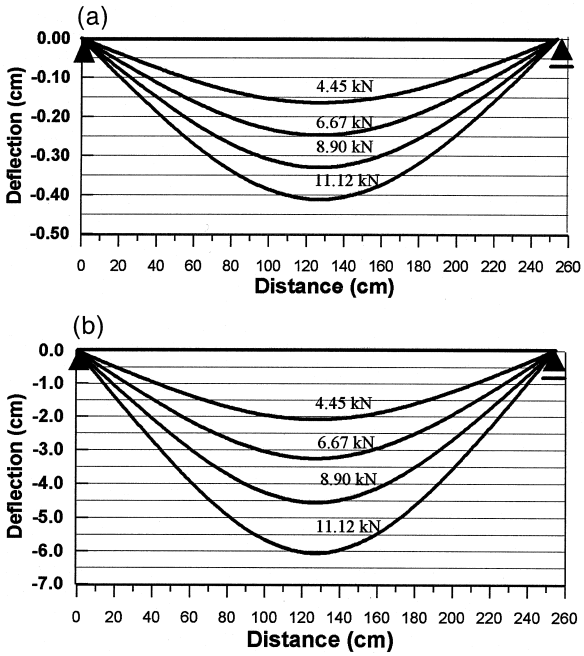

Fig. 10. Deflection of simple beam shown in Fig. 6 due to incremental loading using boron/epoxy composite.

6.2. Statically indeterminate beams

In order to study the effect of material nonlinearity on indeterminate beams, four examples of different beam-configurations are considered, as shown in Fig. 14, including different span lengths and different loading conditions.

6.2.1. Effect of material nonlinearity on bending moments

Before starting the analysis, it is useful to define the redistribution percentage of moment

$$\%M_{\text{red.}} = \frac{M_{\text{q}} - M_{\text{e}}}{M_{\text{e}}} \times 100\% \tag{24}$$

where, M_θ is the value of bending moment at a given location for any fiber orientation θ accounting for nonlinear effect, and M_{e} is the value of bending moment at the same location using linear elastic modulus E_0.

The composite beams, shown in Fig. 14, are subjected to various concentrated loads. The extreme values of bending moments for each load are determined using the present nonlinear analysis method and are compared to those corresponding to the linear analysis method. Figs. 15–18 show the effect of material nonlinearity on the percentage of redistribution of maximum positive and maximum negative bending moments. The position of maximum positive moment is at the middle of the right span, and the maximum negative moment is at the middle support for beams 1, 2, and 3. For Beam 4 there are two values of maximum positive moments, at distances of (72 cm) from left and right supports, respectively.

It is noted from the analysis that, the moment redistributes itself along the beam in a way that the value(s) of larger extreme moment(s) (positive or negative) decreases and the lower extreme moment(s) increases. This is attributed to the nonlinear material behavior of the composite, which at each stress

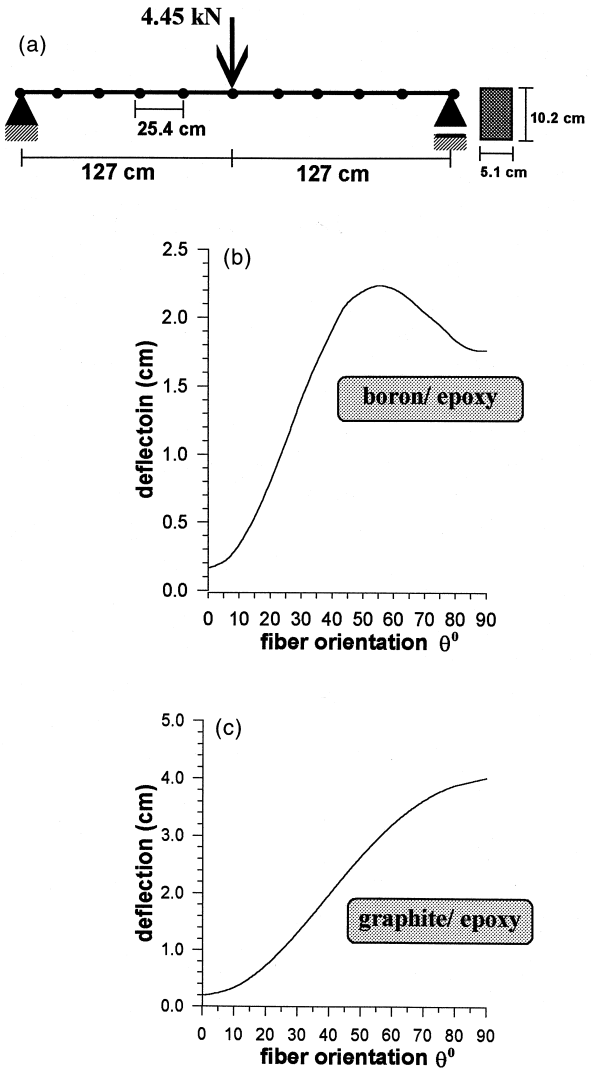

Fig. 11. Midspan deflection vs fiber-orientation for laminated beams made of boron/epoxy and graphite/epoxy.

level on the beam the material possesses a different stiffness. Accordingly, a beam with different stiffnesses is obtained depending on initial moments (at the elastic stage) and hence initial stresses, which leads to stress redistribution along the beam. It is found that, the amount of redistribution increases if the applied load on a given beam increases, and vice versa.

The first three beams, as indicated in Fig. 14 are similar with respect to the loading condition (i.e. the concentrated load is applied at the middle of the second span). The position of the middle support is considered to be variable for the different beams. This movement of the middle support from the left to the right in beams 1, 2, and 3, increases the differences between the maximum positive and maximum negative moments. Referring to Figs. 15–17 and comparing for example, the cases of boron/epoxy beam at $\theta = 20^\circ$ for the three cases, it is obvious that the percentage redistribution of moments is larger when the difference between the positive and negative moments is maximum; as in the case of Beam 3.

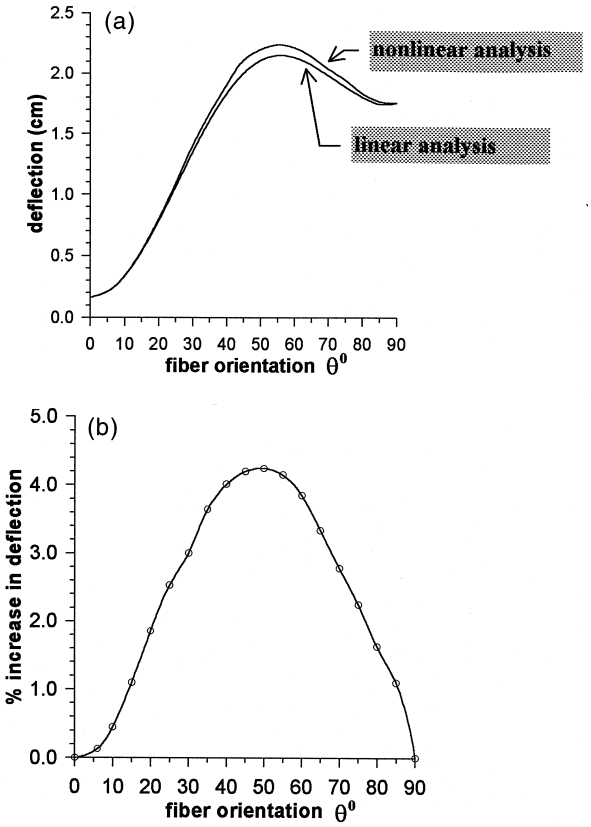

Fig. 12. Comparison between deflections obtained using nonlinear and linear analyses for boron/epoxy.

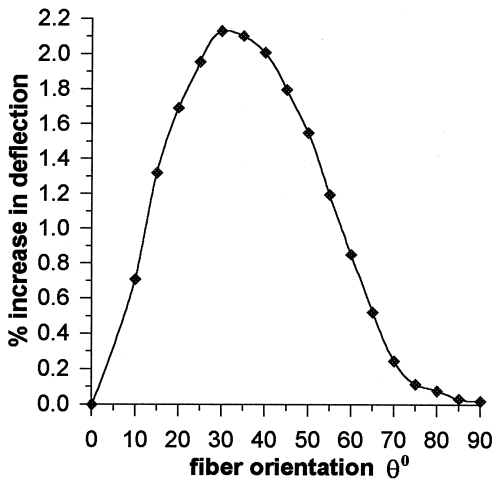

Fig. 13. Perecentage difference between the linear and nonlinear analyses with respect to fiber orientation for graphite/epoxy.

Beam1) $\dfrac{M_{\max}(+ve)}{M_{\max}(-ve)} = 1.5$ (Linear analysis).

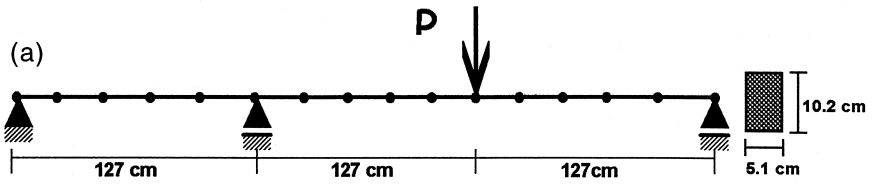

Beam2) $\dfrac{M_{\max}(+ve)}{M_{\max}(-ve)} \approx 2.2$ (Linear analysis).

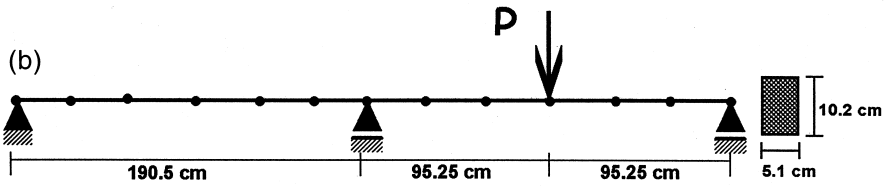

Beam3) $\dfrac{M_{\max}(+ve)}{M_{\max}(-ve)} = 3.5$ (Linear analysis).

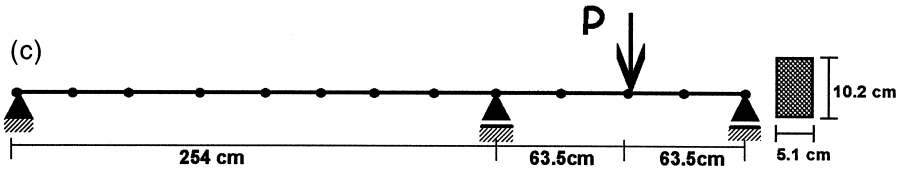

Beam4) $\dfrac{M_{\max}(+ve)}{M_{\max}(-ve)} \approx 0.5$ (Linear analysis).

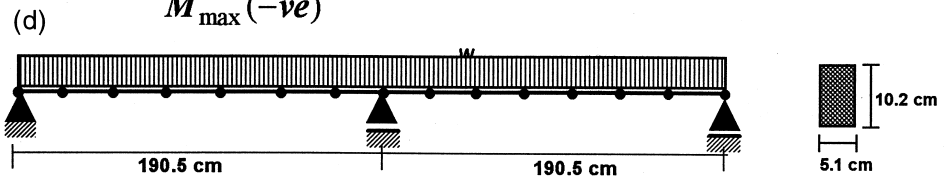

Fig. 14. Schematic representation of the geometry and loading of the different beams.

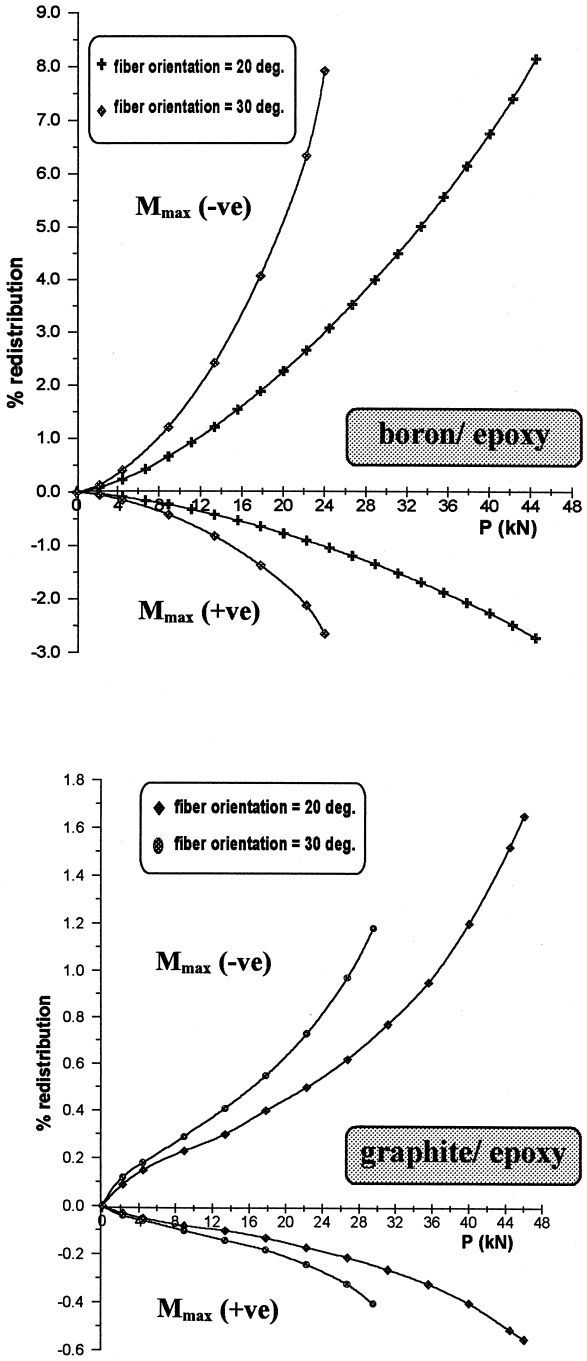

Fig. 15. Percentage redistribution of moment vs applied load for Beam 1 at $\theta = 20$ and 30°.

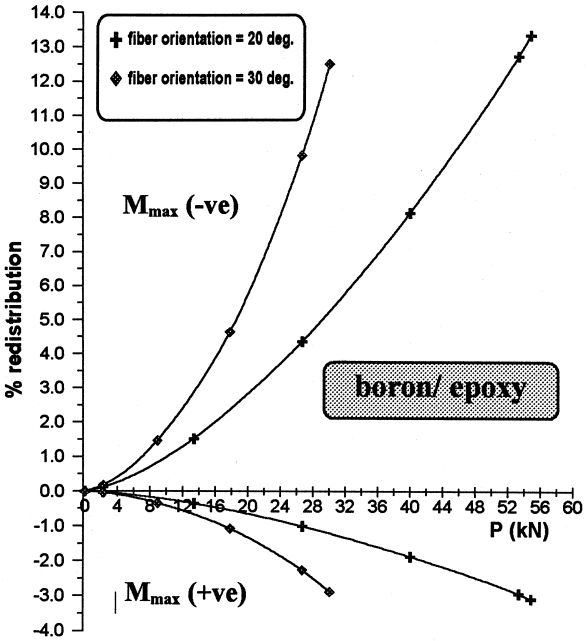

Fig. 16. Percentage redistribution of moment vs applied load for Beam 2 at $\theta = 20$ and 30°.

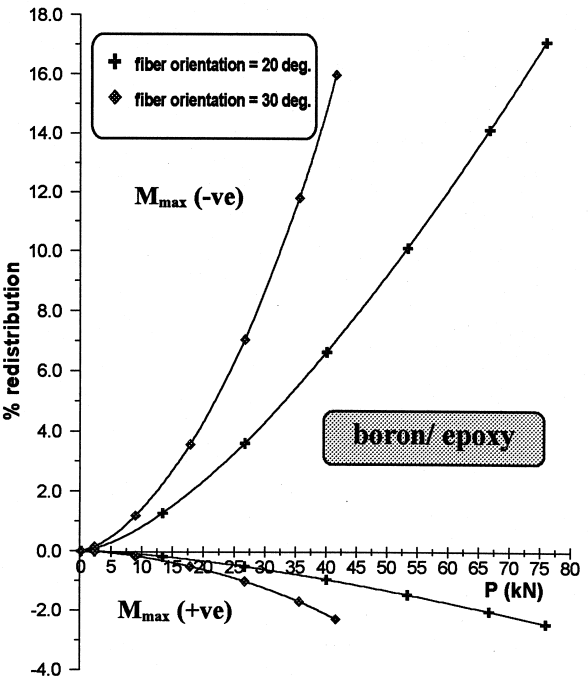

Fig. 17. Percentage redistribution of moment vs applied load for Beam 3 at $\theta = 20$ and 30°.

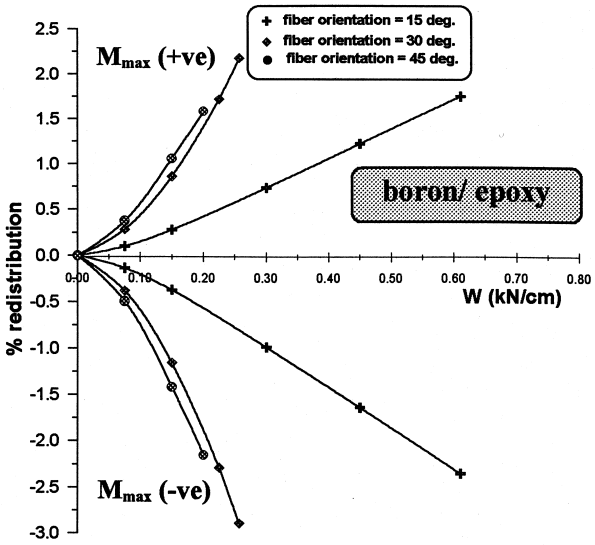

Fig. 18. Percentage redistribution of moment vs applied load for Beam 4 at $\theta = 15$, 30 and 45°.

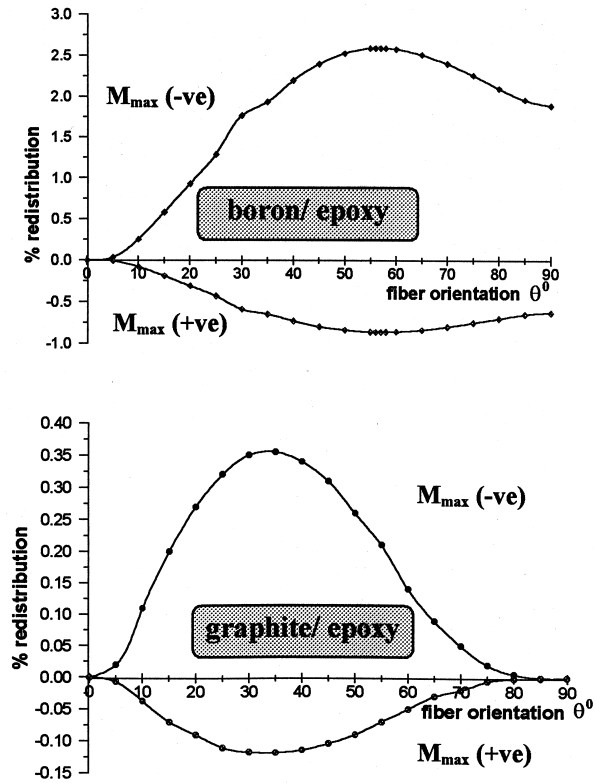

Fig. 19. Effect of fiber orientation on the redistribution of moment in Beam 1 due to applied load of 11.12 kN.

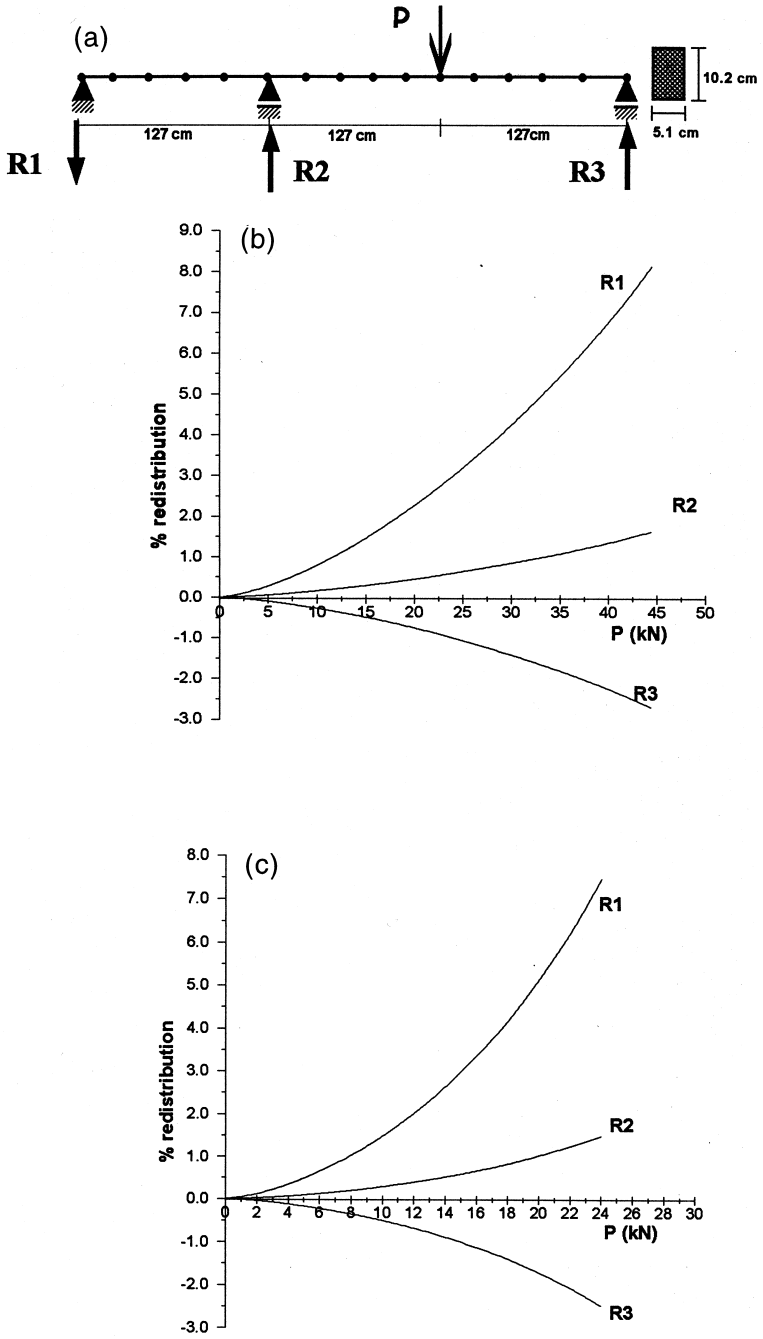

Fig. 20. The percentage redistribution of reactions of Beam 1 due to incrementally applied loads for boron/epoxy composite.

In Beam 4, there is symmetry in loading and geometry which causes the maximum negative moment to be larger than the maximum positive moment. The nonlinear analysis results in an increase in the positive moments in the two spans and a decrease in the negative moment at the location of the middle support. The resulting moment redistribution for boron/epoxy is much lower when compared to the former three cases which is attributed to symmetry of the structure geometry and loading.

6.2.2. Effect of fiber orientation on the redistribution of bending moments

The angle of fiber orientation in a lamina plays a great role in the redistribution of bending moments. To study the fiber orientation effect, Beam 1 in Fig. 14 is subjected to a constant load of 11.12 kN and the fiber-orientation angle (θ) is considered variable. Fig. 19 shows the redistribution percentage of moment for different fiber orientations. It can be noted that for boron/epoxy beams with increasing the fiber-orientation angle, the redistribution of moments increases up to $\theta \approx 56^\circ$, beyond which the redistribution starts to decrease. In graphite/epoxy beams a similar trend appears with a maximum moment redistribution occurs at $\theta \approx 33^\circ$. In general the values of moment redistribution using graphite/epoxy are much smaller than those due to boron/epoxy, which is attributed to the higher material nonlinearity exhibited using boron/epoxy composite.

6.2.3. Effect of material nonlinearity on the reactions

The material nonlinear behavior affects the stress distribution in a beam which in its turn affects moments and then the reactions. Beam 1 is subjected to a load P, and it is analyzed using the present technique. The percentage redistribution in beam reactions versus the applied load P is shown in Fig. 20, where the percentage reaction redistribution is defined as:

$$\%R_{\text{red.}} = \frac{R_{\text{q}} - R_{\text{e}}}{R_{\text{e}}} \times 100\% \tag{25}$$

where R_θ is the reaction value for given fiber orientation (θ) accounting for material non-linearity, and R_{e} is the reaction value using the initial elastic modulus E_0.

As shown in the figure it can be noted that the reactions redistributes themselves; two values increase (R_1 and R_2), and one decrease (R_3) according to the moment distribution along the beam and the location of the supports. This transformation of stresses along the beam naturally satisfies equilibrium, so that the sum of reactions remains unchanged.

7. Conclusions

Material nonlinearity in composites increases the tendency of a given member to deflect, this tendency increases with increasing applied load. In composites, material nonlinearity of the softening type will redistribute the larger moments in indeterminate beam structures. The amount of redistribution depends on the difference between the larger and lower values of the moments; i.e. the bigger the difference is, the larger the redistribution is.

In beams made of boron/epoxy composite, the maximum redistribution occurs at fiber orientation ($\theta \cong 56^\circ$), whereas in graphite/epoxy composite the maximum redistribution occurs at fiber orientation ($\theta \cong 33^\circ$). In general as the angle of fiber orientation (θ) increases in a given composite beam, the stiffness of a given structure decreases and its deflection increases. Material nonlinearity in composites also affects the reactions of a given indeterminate beam, some values of reactions increase and other decrease depending on number and location of supports.

Acknowledgements

This paper is a part of a thesis done by Zoubi, N. R., Civil Engineering Department, at Jordan University of Science and Technology (JUST), 1997.

References

Abu-Farsakh, G., 1989. New material models for nonlinear stress–strain behavior of composite materials. Composites 20 (4), 349–360.

Abu-Farsakh, G., Abdel-Jawad, Y., 1994. A new failure criterion for nonlinear composite materials. Journal of Composites Technology and Research 16 (2), 138–145 JCTRER.

Barbero, J., Lopez-Anido, R., Davalos, J., 1993. On the mechanic of thin-walled laminated composite beams. Journal of Composite Materials 27 (8), 806–829.

Cheung, M.S., Ng, S.F., Bingzhang, Z., 1989. Finite strip analysis of beams and plates with material nonlinearity. Computers and Structures 33 (1), 289–294.

Cole, B., Pipes, R. 1973 Filamentary composite laminate subjected to biaxial stress fields. IIT Research Ins., Chicago, III, and Drexel University, Philadelphia, Pa., Air Force Flight Dynamics Lab. Technical Report AFFDL-TR-73-115.

Fuh-Gwo, Y., Miller, R., 1989. A new finite element for laminated composite beams. Computers and Structures 31 (5), 737–745.

Hahn, H.T., Tsai, S.W., 1973. Nonlinear elastic behavior of unidirectional composite laminae. Journal of Composite Materials 7, 102–118.

Jones, R.M., 1975. Mechanics of Composite Materials. McGraw-Hill Kogakusha, Tokyo.

Meek, J.L., Lin, W.J., 1990. Geometric and material nonlinear analysis of thin-walled beam-columns. Journal of Structural Engineering 116 (6), 1473–1490.

Meek, J.L., Loganathan, S., 1990. Geometric and material non-linear behavior of beam-columns. Computers and Structures 34 (1), 87–100.

Philip, A.T., Karen, C.C., 1988. Stochastic load exceedances with general material nonlinearity. Journal of Structural Engineering 114 (7), 1674–1687.

Prokic, A., 1994. Material nonlinear analysis of thin-walled beams. Journal of Structural Engineering 120 (10), 2840–2852.

Vinson, J., Sierakowski, R., 1986. The Behavior of Structures Composed of Composite Materials. Martinus Nijhof, Dordrecht.

Wong, M.B., Tin-Loi, F., 1990. Analysis of frames involving geometrical and material nonlinearities. Computers and Structures 34 (4), 641–646.

Wu, X.X., Sun, C., 1990. Vibration analysis of laminated composite thin-walled beams systems. AIAA Journal 29, 736–742.